Chemical Engineering Journal 157 (2010) 254–262

Contents lists available at ScienceDirect

Chemical Engineering Journal

journal homepage: www.elsevier.com/locate/cej

The formation of discoid hematite particles from Al-doped ferrihydrite: The effect of trace Fe(II) and the introduction procedures of Al(III)

Hui Liu[a,b,*], Fuling Cao[a], Ping Li[a], Yu Wei[a], Denglu Hou[b,**]

[a] College of Chemistry and Material Science, Hebei Normal University, Shijiazhuang 050016, China
[b] College of Physics Science and Information Engineering, Hebei Normal University, Shijiazhuang 050016, China

ARTICLE INFO

Article history:
Received 17 August 2009
Received in revised form 4 December 2009
Accepted 9 December 2009

Keywords:
Al-doped ferrihydrite
Discoid α-Fe_2O_3
Introduction procedures
Fe(II)

ABSTRACT

The transformation processes from Al-doped ferrihydrites prepared by two procedures (subsequent precipitation (SP) and co-precipitation (CP)) to hematite in the presence or absence of trace Fe(II) have been investigated. The products have been characterized by X-ray diffraction (XRD), scanning electron microscopy (SEM), and X-ray photoelectron spectroscopy (XPS), as well as by a kinetic dissolution process in HCl solution. It was found that Al-doped ferrihydrite prepared by the SP method could be transformed into hematite more easily than that prepared by the CP method in the absence of Fe(II), whereas the opposite was true in the presence of trace Fe(II). The transformation process without Fe(II) was completed through a solid-state transformation mechanism. However, in the transformation process with trace Fe(II), both the dissolution re-precipitation mechanism and the solid-state transformation mechanism operate simultaneously, with the former predominating, especially at a high $n_{Al(III)}/n_{Fe(III)}$ molar ratio. In addition, the present investigation has provided a pathway for the synthesis of discoid Al-doped hematite particles, and the effect of Al^{3+} ions on the formation of discoid hematite particles is also discussed.

1. Introduction

The structural, magnetic, electronic, and catalytic properties of many materials are strongly size/shape dependent at the nanometer level [1]. Therefore, studies on shape-controlled syntheses of nanomaterials are of great interest and are actively being pursued. In fact, as might be expected, α-Fe_2O_3 structures with various morphologies have a wide variety of potential applications, for example in sensors [2,3] or catalysts [4]. To date, hematite particles with various morphologies, such as ellipsoids, rods, tubes, disks, dendrites, flowers, etc., have already been synthesized by various methods [1,5–12]. As for the preparation route in solution, inorganic and organic additives and the acidity of the reaction system appear to be main factors that influence the shape [13]. For example, Ocana et al. [9] studied the formation mechanism of ellipsoidal hematite particles in solution. They proposed that PO_4^{3-} ions were adsorbed on surface planes parallel to the *c* axis of hematite nuclei, which resulted in the growth of anisometric primary particles and producing the final ellipsoidal particles. Sugimoto et al. [14] deduced that the adsorption of chloride and/or chloroferric complexes on the {0 1 2} faces of hematite restrained the growth in the directions normal to the {0 1 2} faces, which resulted in the formation of pseudo-cubic hematite. The adsorption of sulfate ions retarded growth in the directions normal to the c axis and forced the hematite crystals to grow into a peanut shape [15]. Besides inorganic anions, organic additives also can be used as a shape controller to form hematite particles with different shapes. Sugimoto et al. [11] found that 1,4- and 1,2-dihydroxybenzenes could produce ellipsoidal hematite particles, while 1,3-dihydroxybenzene had no effect on the shape of hematite. Gao et al. [16] prepared ellipsoidal hematite particles by introducing glycine. The flower-like α-Fe_2O_3 nanostructures were synthesized by using poly(ethyleneglycol) as a soft-template [17]. Shuttle-like α-Fe_2O_3 nanoparticles were synthesized via a soft-template route using polyethylene glycol (PEG) as polymer, cetyltrimethylammonium bromide (CTAB) as surfactant and $FeCl_3{\cdot}6H_2O$ as iron source materials [18]. Generally speaking, the formation of hematite with different shapes was attributed to the specific adsorption of various additives onto certain crystal faces. In addition, the acidity of the reaction system also significantly affects the morphology of hematite particles. Our earlier results [19] showed that pseudo-cubic hematite particles were obtained at a lower pH (e.g. pH 2) and pseudo-spherical hematite particles were formed at a weak alkaline pH in Cl^- medium. Wang and co-workers [20] explored pH value-dependant growth of α-Fe_2O_3 hierarchical nanostructures. They synthesized two kinds

* Corresponding author at: College of Chemistry and Material Science, Hebei Normal University, Yuhua Road, 113#, Shijiazhuang 050016, China.
Tel.: +86 311 86268342.
** Corresponding author. Tel.: +86 311 86268643.
E-mail addresses: liuhuicn@126.com (H. Liu), houdenglu@mail.hebtu.edu.cn (D. Hou).

1385-8947/$ – see front matter © 2009 Elsevier B.V. All rights reserved.
doi:10.1016/j.cej.2009.12.018

of α-Fe_2O_3 particles, i.e. three-dimensional houseleek-like and two-dimensional snowflake-like dendrites by changing pH value.

It is noteworthy that much research focused on the effect of anions or organic additives on the shape of hematite while relatively little work has been carried out with regard to the influence of the cation. Liu and Osseo-Asare found that aluminum substitution can provide an additional means of shape modification in the production of hematite particles by the sol–gel process [21], whereby peanut-shaped hematite particles were prepared by aging Fe(III) and Al(III) hydroxide suspensions at Al/(Al + Fe) molar ratios of 0.14–0.2 and 100 °C for 8 days. The influence of aluminum was also investigated by Schwertmann, Wolska, and co-workers [22–24]. They found that Al substitution inhibited the growth of hematite in the c-direction.

In recent years, our group has explored the transformation from ferrihydrite to various iron oxyhydroxides or oxides in the presence of trace Fe(II) [25–27]. It has been found that Al-free ferrihydrite could be rapidly transformed into spherical nanosized hematite particles in the presence of trace Fe(II) ($n_{Fe(II)}/n_{Fe(III)} = 0.02$). However, discoid hematite particles were obtained when Al-doped ferrihydrite was used as a precursor. More interestingly, we found that not only was there a great difference in the transformation of co-precipitated and subsequently precipitated Al, Fe hydroxides, but the transformation mechanism in the presence of Fe(II) was also different from that in the absence of Fe(II). Comparing with the results obtained by Liu and Osseo-Asare [21], our transformation time is much shorter than theirs and the morphology of hematite particles is very different. The difference in pH between the two systems is probably responsible for the above results. The aim of this study has been to explore the formation mechanism of discoid Al-substituted hematite particles in both the presence and absence of Fe(II). The results obtained in the present system further indicate the diversity and complexity of iron (hydr)oxide family. Minor change in the experimental condition could probably result in a major change in the morphology of the products. It is prospective that the results in our present investigation would be helpful to the preparation of other metal oxides.

2. Experimental

2.1. Synthesis of samples

All chemicals were analytical grade, purchased from the commercial market, and used without further purification before utilization. The ferric salt ($FeCl_3 \cdot 6H_2O$) solutions were filtered through a 0.22 μm millipore filter to remove any particulate contaminants before utilization.

Al-doped ferrihydrite was prepared by the following two procedures.

(1) NaOH solution (6.0 mol/L) was added dropwise to 50 mL of Fe(III) solution (1.0 mol/L) under vigorous stirring to adjust the pH to 9. A brown slurry was formed (XRD showed the two-line spectrum of ferrihydrite). Subsequently, Al(III) solution ($n_{Al}/n_{Fe(III)} = 0.02–0.14$) was added to the suspension and the pH was again adjusted to 9. The mixture, which was termed "subsequently precipitated Al-doped ferrihydrite" (SP Al-doped ferrihydrite), was stirred for an additional 10 min. Trace Fe(II) solution ($n_{Fe(II)}/n_{Fe(III)} = 0.02$) was then added to the system and the suspension was again adjusted to pH 9 with dilute NaOH solution and at the same time the total volume of the system was adjusted to 100 mL.

(2) 25 mL of Fe(III) solution (2.0 mol/L) was mixed with Al(III) solution (1.0 mol/L, $n_{Al}/n_{Fe(III)} = 0.02–0.14$) and the total volume was adjusted to 50 mL with distilled water. NaOH solution (6.0 mol/L) was added dropwise to the above solution under vigorous stirring to adjust the pH to 9, and the agitation was continued for an additional 10 min. This preparation procedure is termed "co-precipitation" (CP) and the Al-doped ferrihydrite is referred to as "CP Al-doped ferrihydrite". The subsequent procedures were the same as in Procedure 1.

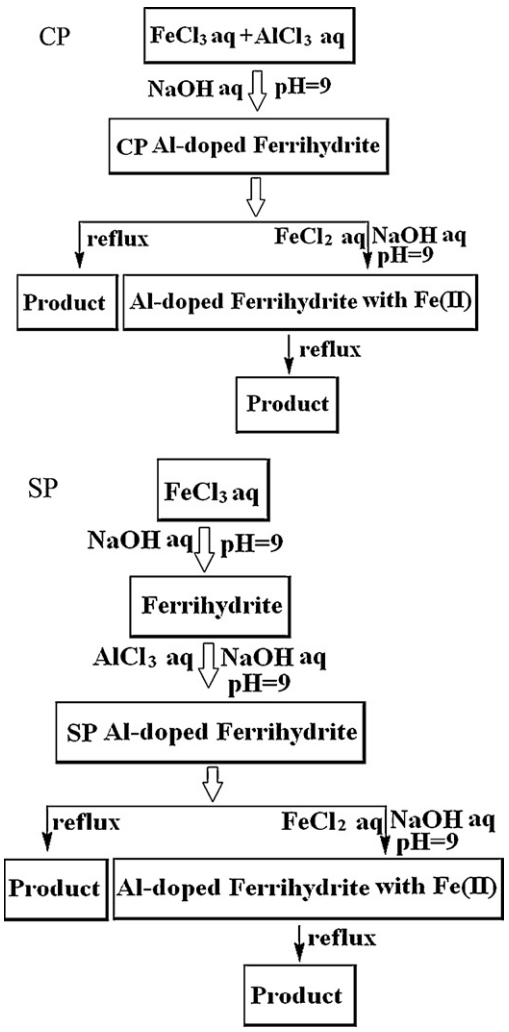

Fig. 1. The schemes of CP and SP procedures.

The experiments were carried out under nitrogen gas and oxygen-free distilled water was used in all stages. The suspensions obtained in the above two systems were heated to boiling and maintained under reflux under vigorous stirring for predetermined times ranging from 1.5 h to 48 h. The products were collected by centrifugation, washed thoroughly with distilled water, and dried at 70–80 °C.

The schemes of the two procedures were shown in Fig. 1.

Dissolution experiment of Al-doped hematite in HCl solution: 0.18 g of Al-doped hematite was added to 150 mL of HCl solution (3.0 mol/L) at 50 °C under vigorous stirring. Aliquots (8 mL) were sampled at specified intervals and centrifuged. The concentrations of Fe(III) and Al(III) ions in the supernatant were determined by means of emission spectrometry (inductively-coupled plasma, ICP).

2.2. Characterization

The powder X-ray diffraction (XRD) was performed by using a Bruker diffractometer D8 ADVANCE equipped with a Cu Kα radi-

ation. Particle size and morphology were determined on a Hitachi H-9000 transmission electron microscopy (TEM) and S-570 scanning electron microscopy. Differential scanning calorimetry (DSC) was performed using a NETZSCH STA 449F3 instrument. DSC curves were recorded by increasing the temperature from room temperature to 800 °C at a rate of 10 °C/min. Al and Fe contents in the products were analyzed with ICP-ULTIMA. X-ray photoelectron spectroscopy (XPS) measurements (MKII VG Company) were employed to gain further insight into the effect of Al ions on the shape of hematite particles.

3. Results and discussion

3.1. The effect of the introduction procedures of Al(III) on the transformation of ferrihydrite

Figs. 2 and 3 show the XRD patterns and SEM images of the products obtained by refluxing SP Al-doped ferrihydrite or CP Al-doped ferrihydrite suspensions for 34 h ($n_{Al}/n_{Fe(III)} = 0.05$). In Fig. 2, all of the reflections of SP sample can be indexed to a pure phase of hematite, and their positions are in good agreement with the literature values (JCPDS No. 33-0664). The narrow, sharp peaks suggest that the hematite product was crystalline. No impurities can be detected from this pattern. Fig. 3SP shows that the hematite was in the form of plate-like particles. The particle shape may be ascribed to the incorporation of Al since no other anions were introduced into the system besides chloride ions [21]. However, only very weak diffraction peaks of hematite can be observed in Fig. 2CP, suggesting an incomplete conversion from CP Al-doped ferrihydrite to hematite after reaction for 34 h. A great deal of amorphous material, which is unconverted Al-doped ferrihydrite, can be observed in Fig. 3CP, suggesting that CP Al-doped ferrihydrite undergoes the desired transformation less readily than SP Al-doped ferrihydrite.

3.2. The effect of the introduction procedures of Al(III) on the transformation of ferrihydrite in the presence of trace Fe(II)

It has been confirmed that Fe(II) adsorbed on ferrihydrite can catalyze the transformation from ferrihydrite to hematite [25]. In fact, catalysis by Fe(II) has also proved to be effective for the transformation of Al-doped ferrihydrite. For example, the transformation time for SP Al-doped ferrihydrite ($n_{Al}/n_{Fe(III)} = 0.06$) in the presence of trace Fe(II) is about 4 h, as compared to only about 1.5 h for CP Al-doped ferrihydrite ($n_{Al}/n_{Fe(III)} = 0.06$). The hematite particles obtained from both SP Al-doped ferrihydrite and CP Al-doped ferrihydrite are spherical (Fig. 4).

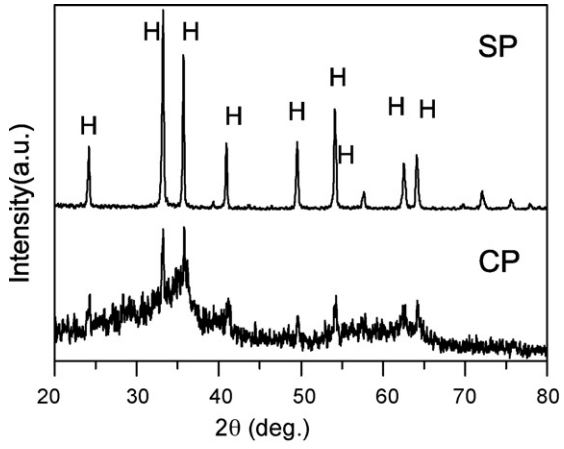

Fig. 2. XRD patterns of the products obtained by SP and CP Al-doped ferrihydrites. $n_{Al}/n_{Fe(III)} = 0.05$, $n_{Fe(II)}/n_{Fe(III)} = 0$, $t = 34$ h. H: hematite.

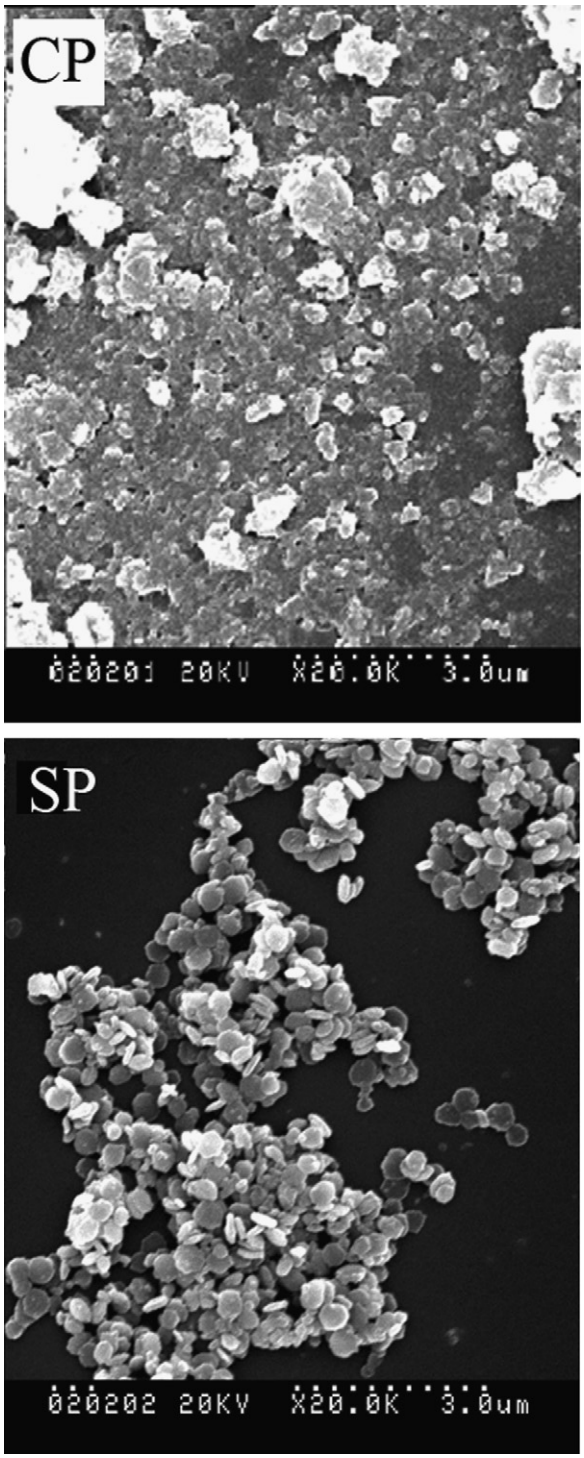

Fig. 3. SEM images of products obtained by SP and CP Al-doped ferrihydrites. $n_{Al}/n_{Fe(III)} = 0.05$, $n_{Fe(II)}/n_{Fe(III)} = 0$, $t = 34$ h.

With increasing Al concentration in Al-doped ferrihydrite, the transformation times for the two Al-doped ferrihydrites are extended (Fig. 5), which indicates that the transformation becomes more difficult. The results from DSC curves of the samples also support this conclusion (Fig. 6). As can be seen in Fig. 6, each DSC curve shows one endothermic and one exothermic peak. The endothermic peak recorded from room temperature to ~200 °C is normally attributed to removal of surface-adsorbed water and water within the structure of Al-doped ferrihydrite [28]. The exothermic peak occurs from 500 to 600 °C, with a different maximum for different

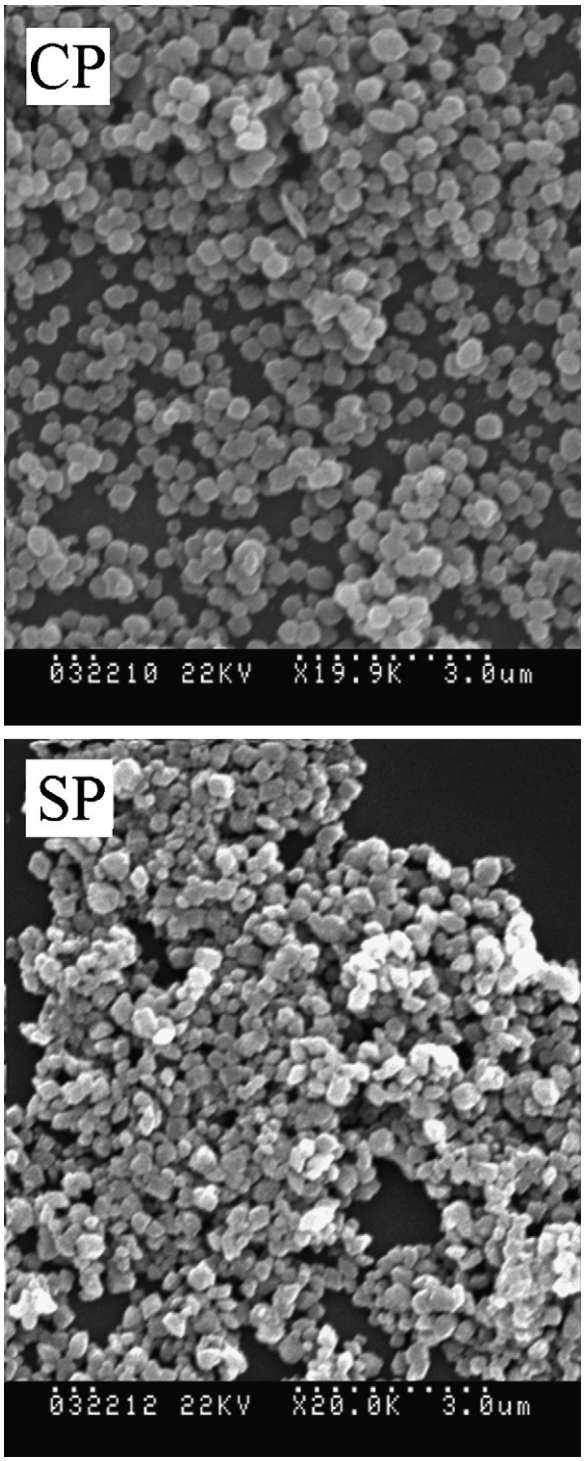

Fig. 4. SEM images of the products obtained by CP and SP Al-doped ferrihydrites in the presence of Fe(II). $n_{Al}/n_{Fe(III)} = 0.06$, $n_{Fe(II)}/n_{Fe(III)} = 0.02$, CP: $t = 1.5$ h, SP: $t = 4$ h.

samples, which is most likely due to the transformation from Al-doped ferrihydrite to hematite. Clearly, with the increasing of the amount of Al, the phase transformation temperatures of Al-doped ferrihydrite increase for both CP and Sp samples, which is consistent with the results in Fig. 5.

However, we noticed that the transformation time of the SP Al-doped ferrihydrite in the presence of Fe(II) was always longer than that of the CP Al-doped ferrihydrite. The higher the level of Al, the more obvious the difference in the transformation times between the two ferrihydrites becomes (Fig. 5). A representative example

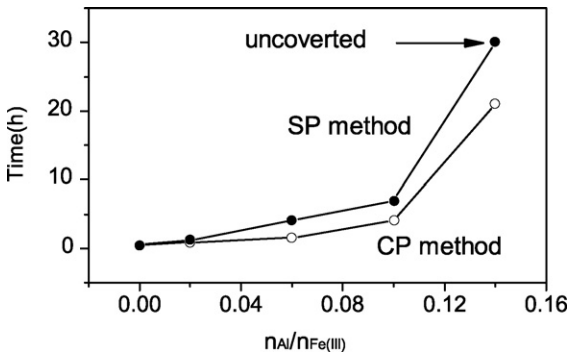

Fig. 5. Changes of transformation time of the two Al-doped ferrihydrites with different Al levels. $n_{Fe(II)}/n_{Fe(III)} = 0.02$.

is shown in Fig. 7. At an $n_{Al}/n_{Fe(III)}$ ratio of 0.14, the transformation product for CP Al-doped ferrihydrite is plate-like hematite particles (Fig. 7CP). The morphology of the product is shown at a high magnification in the inset in Fig. 7CP. It can be seen that these plate-like particles are thicker at their centers than at their outer edges. So it is more accurate to refer to them as discoid particles. However, no obvious change was detected for the SP Al-doped ferrihydrite and the sample remained amorphous (Fig. 7SP).

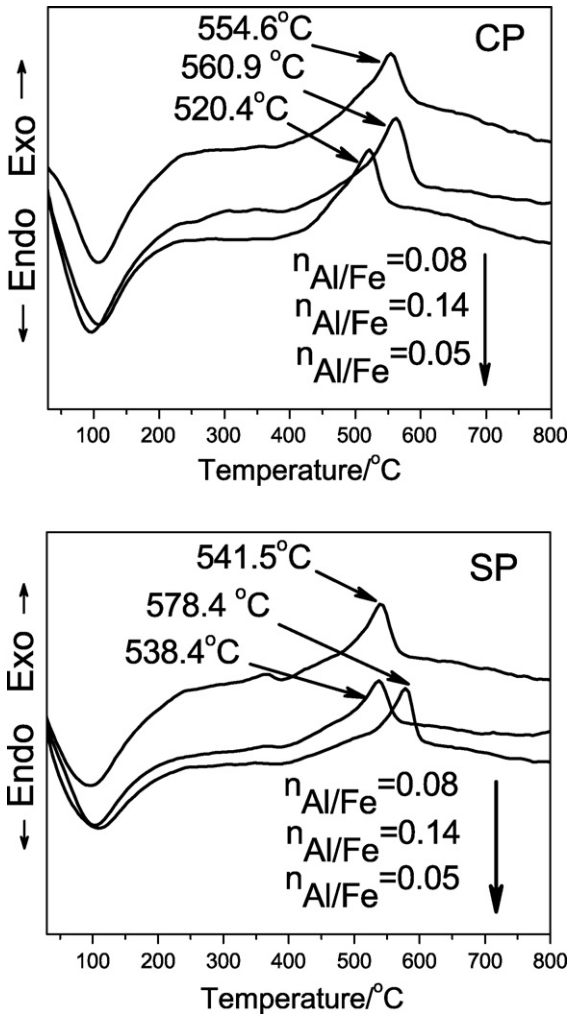

Fig. 6. DSC curves of CP and SP Al-doped ferrihydrites obtained at different $n_{Al}/n_{Fe(III)}$ ratios. $n_{Fe(II)}/n_{Fe(III)} = 0.02$.

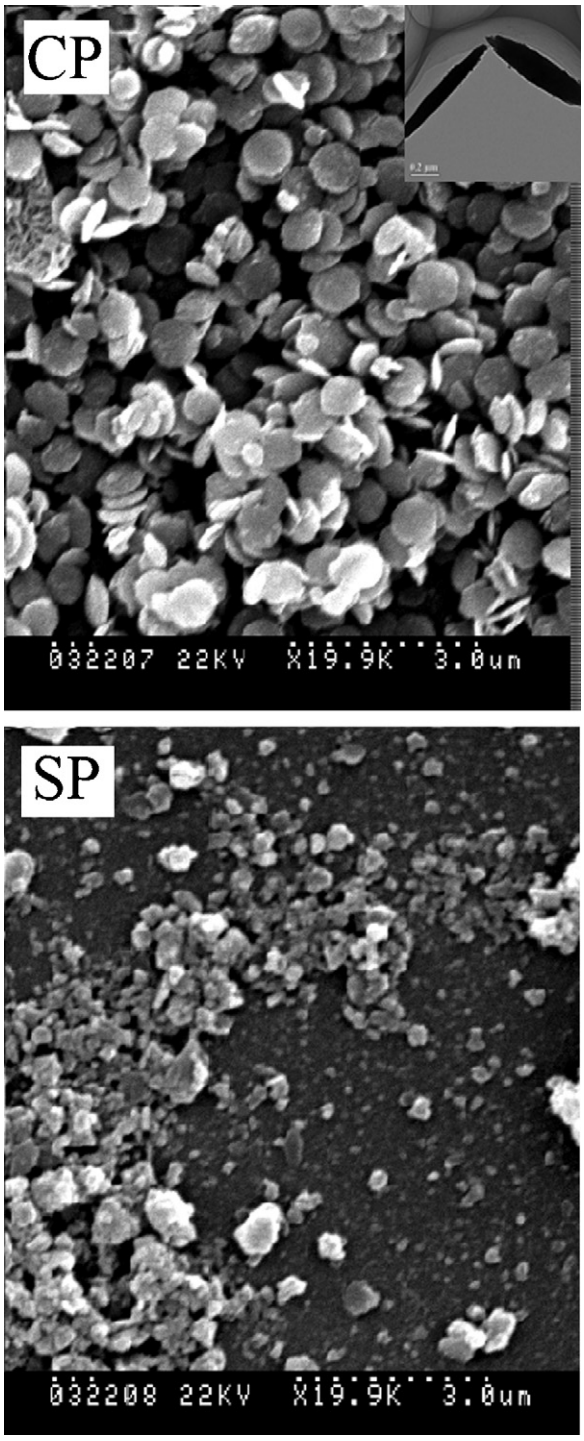

Fig. 7. SEM images of products obtained by CP and SP Al-doped ferrihydrites in the presence of Fe(II). $n_{Al}/n_{Fe(III)} = 0.14$, $n_{Fe(II)}/n_{Fe(III)} = 0.02$, $t = 24$ h.

3.3. The formation mechanism of discoid hematite particles in the presence of Fe(II)

Based on the above results, the order of the transformation rates of SP Al-doped ferrihydrite and CP Al-doped ferrihydrite in the presence of trace Fe(II) is opposite to that in the absence of Fe(II). That is to say, SP Al-doped ferrihydrite transforms into hematite more readily than CP Al-doped ferrihydrite in the absence of Fe(II) but less readily than CP Al-doped ferrihydrite in the presence of Fe(II). These results provide an insight into the mechanism of the transformation in the presence or absence of Fe(II) and highlight the essential effect of Fe(II) acting as a catalyst.

The transformation of ferrihydrite under different conditions is a subject of material science. Proposed mechanisms for the transformation from ferrihydrite to hematite in solution range from dissolution of the precursor followed by precipitation of the product (e.g. the dissolution re-precipitation) to solid-state transformation within precursor aggregates or topotactic transformation accompanied by the phase transformation [29,30]. A pH close to the zero point of charge (zpc) favors the conversion from ferrihydrite to hematite [31]. The solubility of ferrihydrite at this pH reaches a minimum, and a low solubility suppresses the formation of hematite by dissolution re-precipitation and thereby favors the transformation to hematite within the ferrihydrite aggregate, that is, the solid-state transformation.

In the SP method, Fe(III) ions are first precipitated to form ferrihydrite aggregate and then Al(III) ions are deposited on the surface of the ferrihydrite aggregate. The doping of Al onto the ferrihydrite has little influence on the nucleation and growth of hematite particles by solid-state transformation within the ferrihydrite aggregate. The experimental results showed that the transformation time of Al-free ferrihydrite was almost the same as that of Al-doped ferrihydrite at $n_{Al}/n_{Fe(III)} = 0.05$. However, in the CP method, Fe(III) ions and Al(III) ions are co-precipitated, which results in more Al(III) ions being introduced into the interior of the ferrihydrite aggregate. Thus, the nucleation and growth of hematite particles within the ferrihydrite aggregate is affected greatly. The results further support the mechanism of the solid-state transformation from the precursor to product in solution. Fe(II) ions are adsorbed on the surface of Al-doped ferrihydrite aggregate since they are added to the system after the formation of this aggregate. The catalytic effect of Fe(II) on the transformation of ferrihydrite is triggered by interfacial electron transfer to structural Fe(III), which stimulates the dissolution and subsequent re-precipitation or solid-state transformation to a thermodynamically more stable phase. When Fe(II) ions are adsorbed on the surface of SP Al-doped ferrihydrite, the electron transfer between Fe(II) and structural Fe(III) is blocked by the Al ions. On the other hand, according to the literature [32], Al(III), which exists in the form of $Al(OH)_4^-$ at pH 9, readily combines with Fe^{2+} ions due to electrostatic attraction, which also hampers the electron transfer between Fe(II) and structural Fe(III). However, the blocking of electron transfer in the CP Al-doped ferrihydrite system is much less than that in the SP Al-doped ferrihydrite system. Therefore, the nucleation of hematite particles in the SP Al-doped ferrihydrite system is greatly affected and the transformation time is longer than in the CP Al-doped ferrihydrite system. It can thus be concluded that the essential effect of Fe(II) acting as a catalyst should be inducement of the nucleation of hematite. The following diagrammatic sketches (Fig. 8) illustrate the structures of the two Al-doped ferrihydrite aggregates.

Our earlier results revealed that Al-free ferrihydrite was transformed into hematite particles by the catalytic solid-state transformation mechanism at pH 9 and 100 °C within 0.5 h in the presence of Fe(II) [25]. Based on the above analysis, it is known that the solid-state transformation is probably restrained by the presence of Al(III) within the ferrihydrite aggregate in the CP Al-doped ferrihydrite system. The results in Figs. 2 and 3 support this conclusion. Comparing with the SP Al-doped ferrihydrite, the CP Al-doped ferrihydrite is transformed into hematite less readily. We surmise that the transformation of CP Al-doped ferrihydrite in the presence of trace Fe(II) is likely to be completed by the catalytic dissolution re-precipitation mechanism, especially at high levels of Al (e.g. $n_{Al}/n_{Fe(III)} = 0.14$).

In order to investigate the transformation mechanism of the CP Al-doped ferrihydrite in the presence of trace Fe(II), time-dependent experiments were carried out, and the resultant

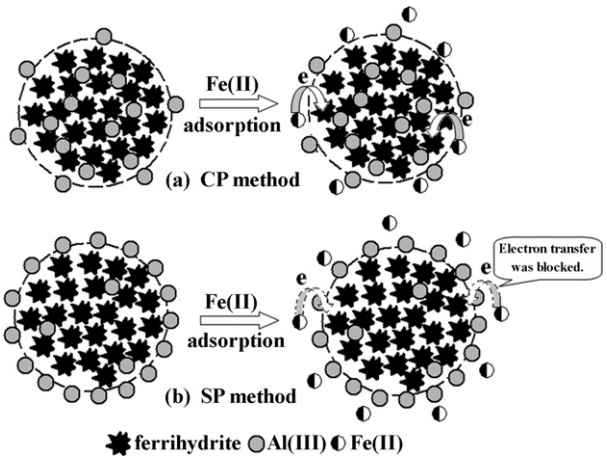

Fig. 8. Diagrammatic sketches of the two Al-doped ferrihydrite aggregates. (a) CP method and (b) SP method.

products were characterized by XRD and SEM investigations. XRD patterns and SEM images as a function of reaction time are recorded. Fig. 9 presents SEM images obtained at different times (XRD patterns not shown). As can be seen in Fig. 9a, hematite appeared after 10 h. Upon prolonging the reaction time to 18 h, discoid hematite particles, co-existing with some amorphous unconverted Al-doped ferrihydrite (Fig. 9b), were observed. The final transformation time was about 21 h (Fig. 9c).

The change in pH during the transformation process provides further information concerning its mechanism. Fig. 10 shows pH vs. time curves for the transformation process in the absence or presence of Al(III). Only a very small pH change (ΔpH) was observed after the transformation of Al-free ferrihydrite (Fig. 10a), which means that the transformation from ferrihydrite to hematite, in this case, was completed mostly by the solid-state transformation mechanism (that is, aggregation–dehydration–rearrangement) [25]. However, the pH decreases by about 4 units for Al-doped ferrihydrite (Fig. 10b). This result indicates that dissolution re-precipitation occurs in the transformation of CP Al-doped ferrihydrite [25,26]. It was confirmed in our previous work that Fe(II), in the form of $FeOH^+$, accelerates the dissolution of ferrihydrite. However, the proportion of $FeOH^+$ ions at pH 9 is so small that the catalytic dissolution rate of ferrihydrite is very slow. Thus, comparing with Al-free ferrihydrite, CP Al-doped ferrihydrite required a much longer time to complete its transformation to hematite by the dissolution re-precipitation mechanism. Clearly, the catalytic dissolution re-precipitation and the catalytic solid-state transformation should occur simultaneously at low $n_{Al}/n_{Fe(III)}$ ratios. The

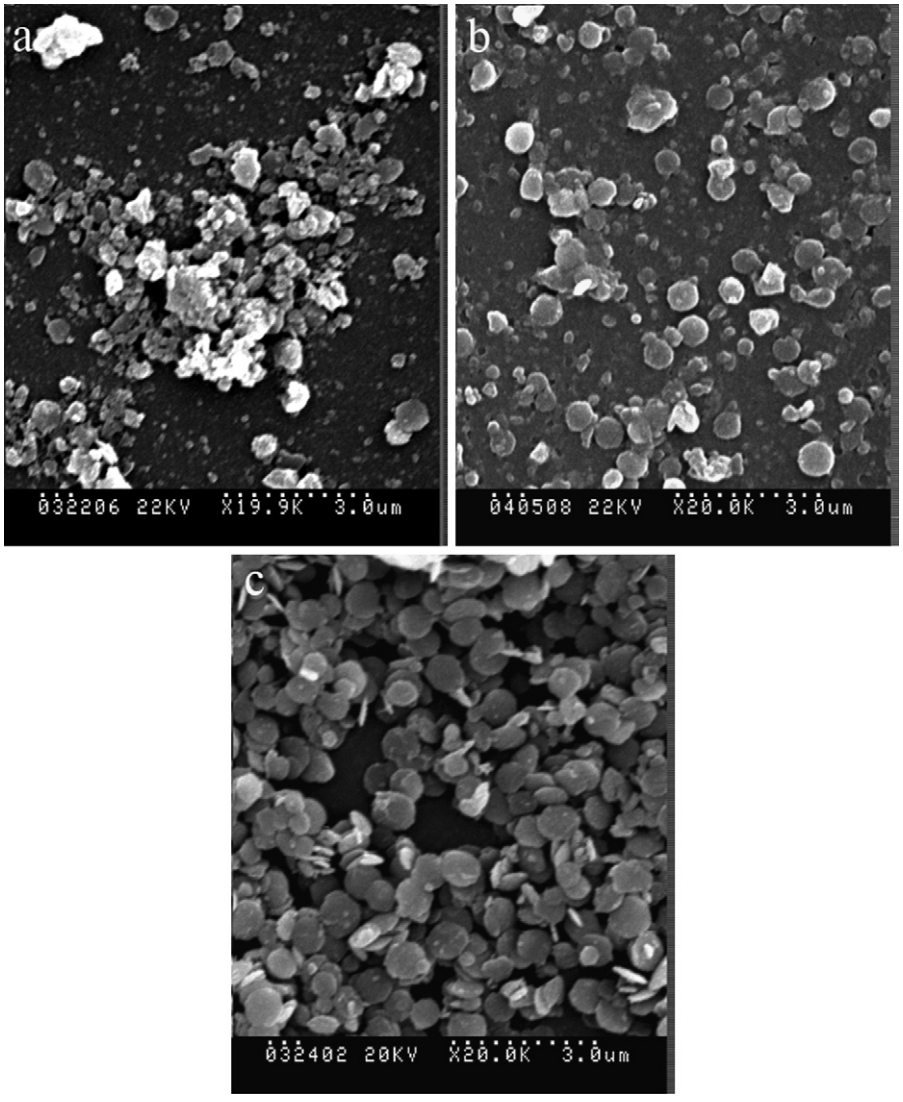

Fig. 9. SEM images of the products obtained by CP Al-doped ferrihydrite at $n_{Al}/n_{Fe(III)} = 0.14$ and $n_{Fe(II)}/n_{Fe(III)} = 0.02$. (a) $t = 10$ h; (b) $t = 18$ h; (c) $t = 21$ h.

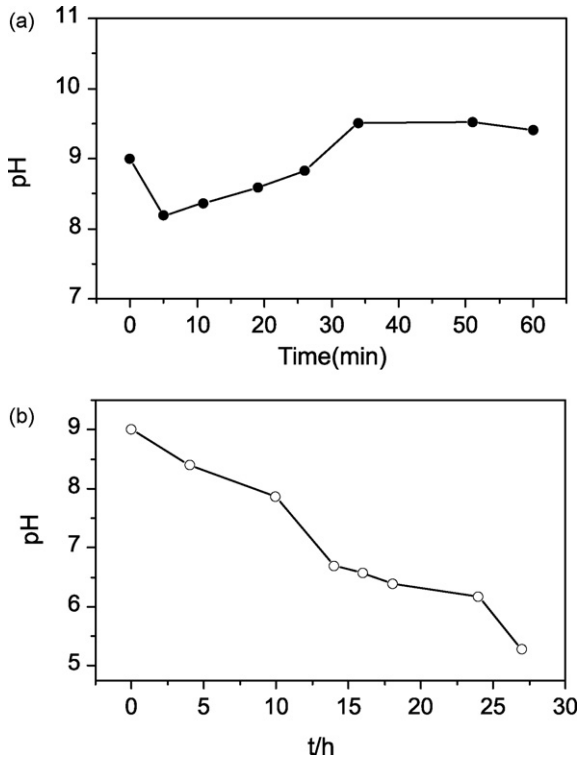

Fig. 10. pH vs. time curves. $n_{Fe(II)}/n_{Fe(III)} = 0.02$, (a) $n_{Al}/n_{Fe(III)} = 0$ and (b) CP method $n_{Al}/n_{Fe(III)} = 0.14$.

higher the Al concentration, the lower the contribution from the solid-state transformation.

To further confirm the above conclusion, two control experiments were designed. In the first, CP Al-doped ferrihydrite was prepared at 60 °C ($n_{Fe(II)}/n_{Fe(III)} = 0.02$ and $n_{Al}/n_{Fe(III)} = 0.14$) and its transformation was studied. No obvious change was detected after reaction for 24 h (XRD pattern not shown). Our earlier experimental results showed that Al(III)-free ferrihydrite prepared at 60 °C was more easily transformed into hematite than ferrihydrite prepared at room temperature (RT) [27]. In addition, it is known that the dissolution will be impaired when ferrihydrite is prepared at a higher temperature [13]. These results mean that Al(III)-free ferrihydrite prepared at 60 °C can transform to hematite through a solid-state transformation mechanism. However, for CP Al-doped ferrihydrite prepared at 60 °C, both the dissolution re-precipitation and the solid-state transformation are restrained, which leads to the above result.

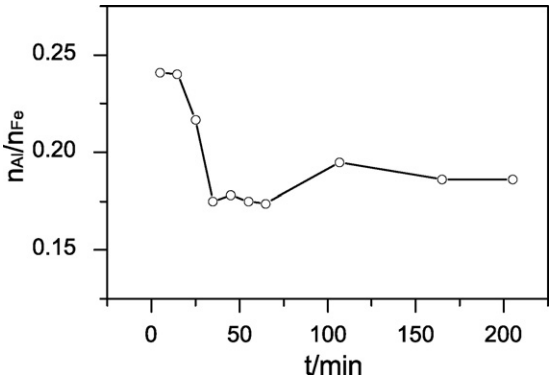

Fig. 11. Changes of $n_{Al}/n_{Fe(III)}$ ratio dissolved into HCl solution with time.

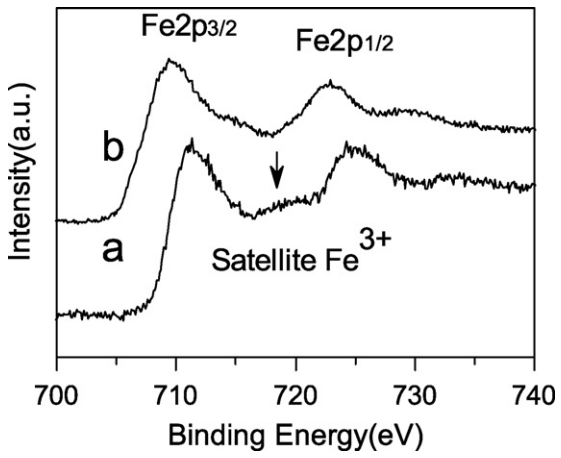

Fig. 12. Fe 2p XPS spectra of as-prepared Al-hematite: (a) without sputtering and (b) after 15 min of sputtering with Ar^+ ions.

For the second control experiment, the initial concentration of Fe(III) in the CP Al-doped ferrihydrite suspension was adjusted to 0.3 mol/L. Complete transformation from CP Al-doped ferrihydrite to hematite was not observed after 24 h (SEM image not shown), which may be attributed to the fact that the concentration of dissolved Fe(III) in the solution at this lower initial concentration was lower than that when 0.5 mol/L was used and hence it was difficult to attain the saturation concentration of Fe(III) for forming hematite.

In order to investigate the effect of Al^{3+} ions on the formation of discoid hematite particles, the as-prepared Al-hematite particles were dissolved in HCl solution under vigorous stirring and the changes in the concentrations of Al^{3+} and Fe^{3+} ions in the solution with time were determined by ICP. The results are shown in Fig. 11. It can be seen that the $n_{Al}/n_{Fe(III)}$ ratio is initially high but gradually decreases with time until it reaches an almost steady level. This result indicates that more Al is incorporated on the surface of hematite particles than is incorporated in their interiors. Al is more easily adsorbed in the direction of the c-axis and retards the crystal growth along this axis, which makes growth along the a- and b-axes relatively favorable. This conclusion is consistent with that reported by Schwertmann et al. [22].

XPS has been employed to analyze the surfaces of the hematite particles as well as their interiors by sputtering the samples with

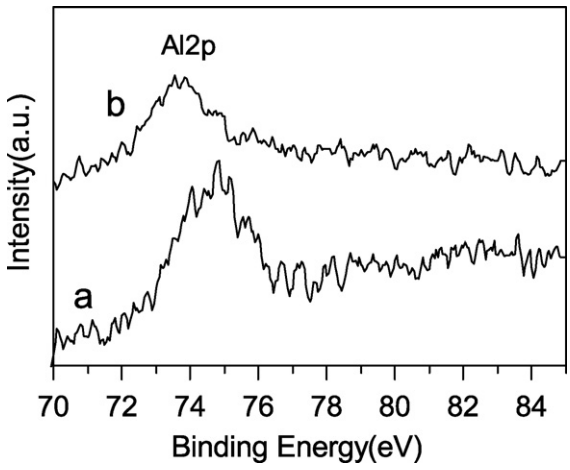

Fig. 13. Al 2p XPS spectra of as-prepared Al-hematite: (a) without sputtering and (b) after 15 min of sputtering with Ar^+ ions.

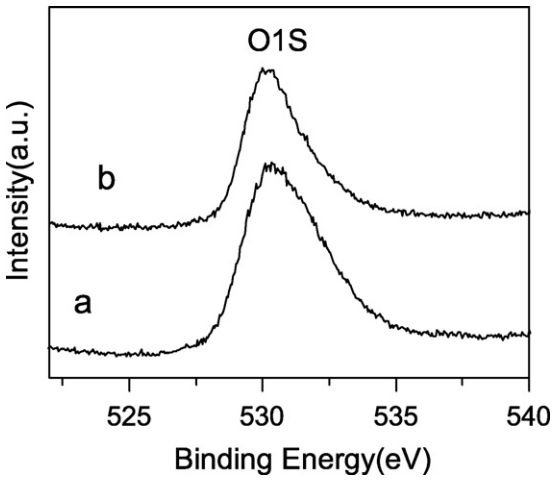

Fig. 14. O 1s XPS spectra of as-prepared Al-hematite: (a) without sputtering and (b) after 15 min of sputtering with Ar^+ ions.

Table 1
Representative XPS binding energy values of different elements in Al-doped hematite sample at the external surface and after 15 min of sputtering with Ar^+ ions of 3 kV.

	BE of XPS signal (eV)		
	Al 2p	Fe $2p_{3/2}$, Fe $2p_{1/2}$	O 1s
No sputtering	74.7	711.4, 724.9	530.6
After sputtering	73.5	709.3, 722.9	530.3

Ar^+ ions for 15 min. Figs. 12–14 show XPS spectra of the as-prepared Al-hematite. In the Fe 2p spectrum (Fig. 12), two peaks at binding energies (BE) of ~711 eV for Fe 2p3/2 and ~724 eV for Fe 2p1/2 with a shake-up satellite at ~719 eV are observed, which is characteristic of Fe(III) in Fe_2O_3 [1]. Peaks at binding energies of ~74 eV for Al 2p and ~530 eV for O 1s are also observed (Figs. 13 and 14). The XPS spectra confirmed that the Al-doped hematite crystals were composed exclusively of Fe, O, and Al.

Table 1 shows representative BE values of the constituent elements of the Al-doped hematite sample, without sputtering and after 15 min of Ar^+ ion sputtering. The shift of the BE line of Al 2p from 74.7 eV to a lower value of 73.5 eV and the shift of the BE lines of Fe 2p from 711.4/724.9 eV to 709.3/722.9 eV after sputtering may suggest that the chemical environments of the Fe and Al ions at the external surface of the particles differ from those in the interiors of the particles. Relative atom concentrations of the different elements in the Al-hematite samples at the external surface without sputtering and after 15 min of sputtering with Ar^+ ions are shown in Table 2. The data in Table 2 indicate that the amount of Al incorporated at the surface of the hematite is greater than that within the hematite particles, which is consistent with the result obtained by ICP. Moreover, the high relative atom concentration of O at the external surface may result from the presence of contaminants and/or OH groups.

Table 2
Relative atom concentration of different elements in Al-hematite samples at the external surface and after 15 min of sputtering with Ar^+ ions of 3 kV.

Region	Surface	After 15 min of sputtering with Ar^+ ions
Al 2p	10.61%	8.45%
Fe 2p	14.66%	39.98%
O 1s	74.74%	51.57%

4. Conclusions

The mechanisms of the transformation from Al-doped ferrihydrite to discoid Al-doped hematite particles in the presence or absence of trace Fe(II) have been investigated. SP Al-doped ferrihydrite transforms to Al-doped hematite particles more rapidly than CP Al-doped ferrihydrite in the absence of Fe(II) and the former transformation is completed mostly by the solid-state transformation mechanism in suspension. CP Al-doped ferrihydrite transforms to Al-doped hematite particles in the presence of trace Fe(II) more rapidly than SP Al-doped ferrihydrite. The CP Al-doped ferrihydrite is mostly transformed by way of the dissolution re-crystallization mechanism in the presence of Fe(II). When CP Al-doped ferrihydrite was used as precursor and Fe(II) was used as a catalyst, discoid hematite particles were obtained. The data from XPS measurements and dissolution experiments on the Al-doped hematite in HCl solution have revealed that the concentration of Al on the surface of the discoid hematite particles was higher than that in the interior of the particles, which indicates that the inclusion of Al provides a method for shape modification in the production of hematite particles.

Acknowledgments

This work was supported by a grant from the Natural Science Foundation of China (20877021) and Ph.D. Programs Foundation and Key Programs of Hebei Normal University (L2005B15 and L2007z06). The authors thank International Science Editing for editing the manuscript.

References

[1] X.L. Hu, J.C. Yu, J.M. Gong, Fast production of self-assembled hierarchical α-Fe_2O_3 nanoarchitectures, J. Phys. Chem. C 111 (2007) 11180–11185.
[2] J. Chen, L.N. Xu, W.Y. Li, X.L. Gou, α-Fe_2O_3 nanotubes in gas sensor and lithium-ion battery applications, Adv. Mater. 17 (2005) 582–586.
[3] Z.Y. Sun, H.Q. Yuan, Z.M. Liu, B.X. Han, X.R. Zhang, A highly efficient chemical sensor material for H_2S: α-Fe_2O_3 nanotubes fabricated using carbon nanotube templates, Adv. Mater. 17 (2005) 2993–2997.
[4] G.P. Escobar, A.Q. Beroy, M.P. Pina Iritia, J.H. Huerta, Kinetic study of the combustion of methyl-ethyl ketone over α-hematite catalyst, Chem. Eng. J. 102 (2004) 107–117.
[5] C.Z. Wu, P. Yin, X. Zhu, C.Z. OuYang, Y. Xie, Synthesis of hematite (α-Fe_2O_3) nanorods: diameter-size and shape effects on their applications in magnetism, lithium ion battery, and gas sensors, J. Phys. Chem. B 110 (2006) 17806–17812.
[6] Y. Wang, H. Yang, Synthesis of iron oxide nanorods and nanocubes in an imidazolium ionic liquid, Chem. Eng. J. 147 (2009) 71–78.
[7] S.Z. Li, H. Zhang, J.B. Wu, X.Y. Ma, D.R. Yang, Shape-control fabrication and characterization of the airplane-like FeO(OH) and Fe_2O_3 nanostructures, Cryst. Growth Des. 6 (2006) 351–353.
[8] S.B. Wang, Y.L. Min, S.H. Yu, Synthesis and magnetic properties of uniform hematite nanocubes, J. Phys. Chem. C 111 (2007) 3551–3554.
[9] M. Ocana, M.P. Morales, C.J. Serna, The growth mechanism of α-Fe_2O_3 ellipsoidal particles in solution, J. Colloid Interface Sci. 171 (1995) 85–91.
[10] B. Tang, G.L. Wang, L.H. Zhuo, J.C. Ge, L.J. Cui, Facile route to α-FeOOH and α-Fe_2O_3 nanorods and magnetic property of α-Fe_2O_3 nanorods, Inorg. Chem. 45 (2006) 5196–5200.
[11] T. Sugimoto, H. Itoh, T. Mochida, Shape control of monodisperse hematite particles by organic additives in the gel–sol system, J. Colloid Interface Sci. 205 (1998) 42–52.
[12] H. Park, P. Ayala, M.A. Deshusses, A. Mulchandani, H. Choi, N.V. Myung, Electrodeposition of maghemite (γ-Fe_2O_3) nanoparticles, Chem. Eng. J. 139 (2008) 208–212.
[13] R.M. Cornell, U. Schwertmann, The Iron Oxides, VCH Publishers, New York, 2003.
[14] T. Sugimoto, K. Sakata, A. Muramatsu, Formation mechanism of monodisperse pseudocubic α-Fe_2O_3 particles from condensed ferric hydroxide gel, J. Colloid Interface Sci. 159 (1993) 372–382.
[15] T. Sugimoto, Y.S. Wang, Mechanism of the shape and structure control of monodispersed α-Fe_2O_3 particles by sulfate ions, J. Colloid Interface Sci. 207 (1998) 137–149.
[16] C.Q. Hu, Z.H. Gao, X.R. Yang, Facile synthesis of single crystalline α-Fe_2O_3 ellipsoidal nanoparticles and its catalytic performance for removal of carbon monoxide, Mater. Chem. Phys. 104 (2007) 429–433.
[17] Y.N. NuLi, P. Zhang, Z.P. Guo, P. Munroe, H. Liu, Preparation of α-Fe_2O_3 submicro-flowers by a hydrothermal approach and their electrochemical

performance in lithium-ion batteries, Electrochim. Acta 53 (2008) 4213–4218.
[18] X.M. Liu, S.Y. Fu, H.M. Xiao, C.J. Huang, Preparation and characterization of shuttle-like α-Fe_2O_3 nanoparticles by supermolecular template, J. Solid State Chem. 178 (2005) 2798–2803.
[19] H. Liu, Y. Wei, Y.H. Sun, W. Wei, Dependence of the mechanism of phase transformation of Fe(III) hydroxide on pH, Colloids Surf. A 252 (2005) 201–205.
[20] C. Jia, Y. Cheng, F. Bao, D.Q. Chen, Y.S. Wang, pH value-dependant growth of α-Fe_2O_3 hierarchical nanostructures, J. Cryst. Growth 294 (2006) 353–357.
[21] Q.Y. Liu, K.J. Osseo-Asare, Al-substituted hematite particles from highly condensed metal hydroxide gels, J. Colloid Interface Sci. 231 (2000) 401–403.
[22] U. Schwertmann, R.W. Fitzpatrick, R.M. Taylor, D.G. Lewis, The influence of aluminum on the iron oxides. Part II. Preparation and properties of Al-substituted hematites, Calys Clay Min. 27 (1979) 105–112.
[23] U. Schwertmann, J. Friedl, H. Stanjek, D.G. Schulez, The influence of aluminum on the iron oxides. Part XIX. Formation of Al-substituted hematites from ferrihydrite at 25 °C and pH 4 to 7, Calys Clay Min. 48 (2000) 159–172.
[24] E. Wolska, W. Szajda, Temperature effects on coprecipitated Al, Fe-hydroxides during hydrothermal transformation, J. Therm. Anal. 32 (1987) 797–805.
[25] H. Liu, Y. Wei, Y.H. Sun, The formation of hematite from ferrihydrite using Fe(II) as a catalyst, J. Mol. Catal. A: Chem. 226 (2005) 135–140.
[26] H. Liu, P. Li, M.Y. Zhu, Y.H. Sun, Fe(II)-induced transformation from ferrihydrite to lepidocrocite and goethite, J. Solid State Chem. 180 (2007) 2121–2128.
[27] H. Liu, P. Li, B. Lu, Y. Wei, Y.H. Sun, Transformation of ferrihydrite in the presence or absence of trace Fe(II): the effect of preparation procedures of ferrihydrite, J. Solid State Chem. 182 (2009) 1761–1771.
[28] F.M. Michel, L. Ehm, G. Liu, W.Q. Han, S.M. Antao, P.J. Chupas, P.L. Lee, K. Knorr, H. Eulert, J. Kim, C.P. Grey, A.J. Celestian, J. Gillow, M.A.A. Schoonen, D.R. Strongin, J.B. Parise, Similarities in 2- and 6-line ferrihydrite based on pair distribution function analysis of x-ray total scattering, Chem. Mater. 19 (2007) 1489–1496.
[29] A. Manceau, V.A. Drits, Local structure of ferrihydrite and feroxyhite by EXAFS spectroscopy, Clay Miner. 28 (1993) 165–184.
[30] R.M. Cornell, W. Schneider, Phase transformations in the ferrihydrite/cysteine system, Polyhedron 8 (1989) 2829–2836.
[31] U. Schwertmann, J. Friedl, H. Stanjek, From Fe(III) ions to ferrihydrite and then to hematite, J. Colloid Interface Sci. 209 (1999) 215–223.
[32] M.P. Walsh, L.W. Lake, Description of chemical precipitation mechanisms and their role in formation damage during stimulation by hydrofluoric acid, J. Petrol. Technol. (1982) 10625.